Forest Ecology and Management 351 (2015) 67–77

Contents lists available at ScienceDirect

Forest Ecology and Management

journal homepage: www.elsevier.com/locate/foreco

Empirical models for tracing seasonal changes in leaf area index in deciduous broadleaf forests by digital hemispherical photography

Zhili Liu [a], Chuankuan Wang [a], Jing M. Chen [b], Xingchang Wang [a], Guangze Jin [a,*]

[a] Center for Ecological Research, Northeast Forestry University, Harbin 150040, China
[b] Department of Geography, University of Toronto, Toronto, ON M5S 3G3, Canada

ARTICLE INFO

Article history:
Received 13 December 2014
Received in revised form 3 May 2015
Accepted 5 May 2015
Available online 19 May 2015

Keywords:
Leaf area index
Seasonal variations
Digital hemispherical photography (DHP)
Litter collection
Regression
Error sources

ABSTRACT

Accurate estimation of seasonal leaf area index (LAI) variations is essential for predicting forest growth, but rapid and reliable methods for obtaining such estimates have rarely been reported. In this study, direct measurements of LAI seasonal variations in deciduous broadleaf forests in China were made through leaf seasonality observations in the leaf-out season and litter collection in the leaf-fall season. Meanwhile, indirect LAI measurements were made using a digital hemispherical photography (DHP) method. Our objectives were to explore the relationship between direct and indirect LAI measurements and to recommend a rapid and reliable method to determine the seasonal variation of LAI in forests. To achieve these objectives, we first evaluated seasonal variations of the biases due to key factors (woody materials, clumping effects and incorrect automatic exposure) known to influence the estimation of LAI by DHP. The results showed that the biases due to these factors exhibited different seasonal variation patterns, and the total contribution of these factors could explain 72% of the difference between direct LAI and DHP LAI throughout the entire growing season. Second, linear regression models between direct and DHP LAI were first constructed for each 10-day period as well as the entire growing season. Significance tests were made to the differences among the models for different dates, and models for estimating LAI based on DHP in each date were aggregated to 4 periods with R^2 and RMSE values of 0.91 and 0.22, 0.79 and 0.29, 0.81 and 0.14, 0.97 and 0.14, respectively. There was no significant difference between direct LAI and estimated LAI using the four models in each aggregated period ($p < 0.01$). Thus, we confirm that these models can fully simulate the seasonal variations in LAI from the initial leaf emergence to leaf fall in deciduous broadleaf forests.

1. Introduction

Leaf area index (LAI), defined as one half the total green leaf area per unit ground surface area (Chen and Black, 1992), is a central parameter for analyses of forest canopies, which affect the energy, water and carbon fluxes between the canopies and the atmosphere (Asner et al., 2003; Bréda, 2003; Ryu et al., 2012). Furthermore, the seasonal changes in LAI strongly influence the variations in the rates of many forest ecosystem processes such as rain interception, evapotranspiration, photosynthesis and respiration, and LAI has also been used as a predictor for many processes useful for forest management (Arias et al., 2007; Richardson et al., 2011; Sprintsin et al., 2011).

LAI can be obtained directly by destructive sampling, but this method is not only destructive but also unsuitable for forest stands with high and complicated canopies (Chen et al., 1997; Gower et al., 1999; Jonckheere et al., 2004). In contrast, allometric methods are less destructive, and LAI estimates are often based on the development of allometric relationships between LAI and tree data (e.g., diameter at breast height (DBH), sapwood cross-sectional area or basal area) (Gower and Norman, 1991; Jonckheere et al., 2005; Majasalmi et al., 2013). However, these relationships are both species- and site-specific, and these methods cannot be used to monitor the seasonal changes in LAI of a forest stand (Smith et al., 1993; Chen and Cihlar, 1995a; Küßner and Mosandl, 2000). As an alternative to measure LAI directly, the litter collection method has frequently been used in deciduous forests (Neumann et al., 1989; Ishihara and Hiura, 2011). Recently, Nasahara et al. (2008) proposed a method that combines litterfall in the leaf-fall season with leaf seasonality observations in the leaf-out season to monitor the seasonal changes in LAI in a deciduous broadleaf forest. However, the litter collection method used to derive LAI requires multiplying the collected mass of leaves by the specific

* Corresponding author. Tel.: +86 451 82191823.
E-mail address: taxus@126.com (G. Jin).

http://dx.doi.org/10.1016/j.foreco.2015.05.005
0378-1127/

leaf area (SLA), which must be determined for each tree species separately (Kalácska et al., 2005; Nouvellon et al., 2010). Meanwhile, litterfall should be collected and sorted by species promptly to avoid leaf decomposition.

Because these direct methods for measuring LAI are time-consuming and labor-intensive for forest canopies, a number of indirect techniques relying on radiative transfer theories have been developed to infer LAI from measurements of the transmission of radiation through a canopy (Ross, 1981). In these techniques, digital hemispherical photography (DHP) and the LAI-2000 plant canopy analyzer (Licor Inc., Lincoln, NE, USA) have usually been used to measure LAI because they can simultaneously measure the canopy gap fraction from several zenith angles. With the development of high-resolution digital cameras, accurate and effective processing of images and permanent preservation of original field data, DHP has been widely accepted as a tool for measuring LAI by forest managers and researchers (Chen et al., 1997; van Gardingen et al., 1999; Gonsamo and Pellikka, 2009; Leblanc and Fournier, 2014). Nevertheless, the accuracy of these indirect LAI estimates should be checked against direct measurements of LAI because of the methods' inherent limitations. For instance, indirect methods cannot fully distinguish woody materials and leaves in the process of calculating the canopy gap fraction and LAI (Chen et al., 1991; Bréda, 2003); they infer LAI under the assumption that the foliage components are distributed randomly in canopies, but most canopies exhibit clumping patterns (Black et al., 1991; Chen et al., 1997). Therefore, this LAI directly derived from indirect methods (i.e., optical methods) is not the true LAI but rather an effective LAI (L_e) (Chen, 1996). Recently, automatic exposure setting has been identified as a large source of error in estimating LAI using DHP because it often causes significant loss of green leaves in the photographs (Zhang et al., 2005; Chianucci and Cutini, 2012; Beckschäfer et al., 2013; Macfarlane et al., 2014).

To the best of our knowledge, rapid and accurate monitoring of the seasonal changes in LAI based on field measurements in a forest stand could most likely be accomplished in two ways: 1, based on the indirect LAI, we could estimate the direct LAI by constructing relationships between indirect and direct LAI in different seasons; or 2, we could correct the indirect LAI estimates by accounting for factors that influence the accuracy of LAI estimation (e.g., woody materials or clumping effects) in different seasons. However, consensus methods for quantifying these factors have not been developed. Even if we obtained the corrected indirect LAI in different seasons, its accuracy would still need to be checked against direct estimates of LAI. In contrast, the first way of monitoring the seasonal changes in LAI is more practical and effective, as reported by many previous studies. For instance, Chason et al. (1991) estimated the seasonal dynamics of LAI using LAI-2000 and litter collection measurements in a mixed deciduous broadleaf forest and found that $LAI_{litter} = 1.86 \times LAI_{LAI\text{-}2000}$ with $R^2 = 0.97$; Kalácska et al. (2005) reported the seasonal changes in LAI derived from optical (e.g., LAI-2000) and litter collection methods in a tropical dry forest and constructed a relationship of $LAI_{litter} = 2.12 \times LAI_{LAI\text{-}2000} - 1.55$ ($R^2 = 0.78$). However, whether a single model is useful across different seasons has not been assessed in most of these studies. Qi et al. (2013) constructed the relationship between the effective LAI from DHP and direct LAI in the leaf-fall season in a mixed broadleaved-Korean pine forest in China, but detail for the leaf-out season is lacking. Up to now, few studies have constructed a time-dependent relationship between direct LAI and indirect LAI from initial leaf-out to the leaf-fall season in a forest stand.

This study aims to develop accurate but less labor-intensive empirical models to determine the seasonal changes in LAI using the indirect DHP method in deciduous broadleaf forests. To achieve this aim, we (1) evaluated the seasonal variations of the biases due to error sources of LAI measurement by DHP (e.g., woody materials, clumping effects or photographic exposure); (2) directly measured the seasonal changes in LAI (defined as direct LAI) by combining leaf seasonality observations in the leaf-out season with litter collection in the leaf-fall season; and (3) constructed an empirical model based on the correlation between direct LAI and indirect LAI in each 10-day period and explored how to integrate these models in all dates.

2. Materials and methods

2.1. Site description and sample design

The study site is at the Maoershan Ecosystem Research Station of Northeast Forestry University in northeastern China (127°30′–34′E, 45°20′–25′N). It represents typical deciduous forest in northeastern China, with an average altitude of 300 m above sea level and an average slope of 10°–15°. The mean (1989–2009) annual precipitation is 629 mm, of which ~50% falls between June and August. The mean annual air temperature is 3.1 °C. The frost-free period spans between 120 d and 140 d, with an early frost in September and a late frost in May (Wang et al., 2013). The study was conducted using four 20 m × 30 m permanent plots of mixed deciduous broadleaf plants, the basic characteristics of which are summarized in Table 1. We randomly installed five litter traps in each plot (i.e., a total of 20 l traps). Each trap had a square aperture of 1 m^2 and a base approximately 0.5 m above the ground. Observations were recorded from May 1 to October 21 of 2012, and there were nearly no leaves on trees before May 1 and after October 21, i.e., the LAIs in these two dates were zero. Therefore, the entire growing season in this study area contains leaf-out seasons and leaf-fall seasons, and the leaf-out season is from May 12 to mid-July when the annual maximum LAI, LAI_{max} occurred, and the leaf-fall season is from August 1 to October 11.

2.2. Indirect LAI estimation

We used a DHP technique (with a Nikon Coolpix 4500 digital camera with a 180° fish-eye lens) to estimate LAI on the same dates as the leaf seasonality observations and litter collection dates. All of the hemispherical photographs of sample points were taken 1.3 m above the ground using a tripod, and the sample points were located near litter traps. The photographs were obtained near sunrise (or sunset) under uniform sky conditions. We chose the following settings for the camera: (1) aperture priority mode with

Table 1
General characteristics and species composition of the four deciduous broadleaf forest plots under investigation.

Forest plots	Major species	Density trees (ha^{-1})	Mean DBH (cm)	Basal area ($m^2\ ha^{-1}$)	Height (m)
1	*Ulmus japonica* (64.8%), *Fraxinus mandshurica* (15.8%)	1840	7.73	19.59	20
2	*Betula platyphylla* (47.9%), *Ulmus japonica* (20.3%)	2140	8.01	19.64	18
3	*Betula platyphylla* (50.8%), *Acer mono* (7.3%)	5067	6.29	23.25	16
4	*Fraxinus mandshurica* (49.5%), *Ulmus japonica* (32.5%)	2167	9.09	35.94	21

Values in parentheses are dominance (i.e., the proportion of the total basal area of all species in the plot represented by the basal area of major species) of species; DBH stands for diameter at breast height. Height is a canopy height of the dominant species in each plot.

aperture set at F 5.3 (i.e., automatic exposure); (2) high image quality (2272 × 1704 Pixels); and (3) Fine JPEG format. A total of 340 hemispheric photographs were obtained at four plots over all study dates (from May 1 to October 21). Based on the theorem of Miller (1967), a method for calculating effective LAI (L_e) by optical methods (e.g., DHP) can be applied (Chen, 1996):

$$L_e = -2\int_0^{\pi/2} \ln[P(\theta)]\cos\theta\sin\theta d\theta \quad (1)$$

where $P(\theta)$ is the canopy gap fraction at zenith angle θ averaged for an image. In this study, the hemispherical photographs were processed with DHP software to derive L_e, i.e., DHP L_e (Leblanc et al., 2005; Chianucci et al., 2015), with zenith angle ranges of 30°–60° (Gonsamo and Pellikka, 2009).

2.3. Bias analysis of indirect optical LAI estimation

Based on previous theoretical development and validation (Chen et al., 1997), the following governing equation was used to obtain more accurate LAI estimates based on L_e by:

$$\mathrm{LAI} = \frac{(1-\alpha)L_e\gamma_E}{\Omega_E} \quad (2)$$

where α is the woody-to-total area ratio, representing the contribution of woody materials to L_e; Ω_E is the clumping index, quantifying the effect of foliage clumping beyond shoots level; and γ_E is the needle-to-shoot area ratio, quantifying the effect of foliage clumping within shoots. For broadleaf species, individual leaves are considered as foliage elements, and $\gamma_E = 1.0$. Additionally, the accuracy of LAI measured using the DHP method is affected by an additional issue of automatic exposure setting (quantified by E). Therefore, for the DHP method in this study, the biases of LAI measurement were caused by α, Ω_E, and E, thus, LAI = f_{DHP} (α, Ω_E, E). Then, we calculated the total bias (ΔLAI) (Topping, 1972):

$$\Delta\mathrm{LAI} = \frac{\partial\mathrm{LAI}}{\partial\alpha}\times\Delta\alpha + \frac{\partial\mathrm{LAI}}{\partial\Omega_E}\times\Delta\Omega_E + \frac{\partial\mathrm{LAI}}{\partial E}\times\Delta E \quad (3)$$

where $\Delta\alpha = 0 - \bar{\alpha}$; $\Delta\Omega_E = 1 - \bar{\Omega_E}$; and $\Delta E = 1 - \bar{E}$.

In this study, we used two schemes to calculate the α value for each date during the entire growing season. Scheme A: We obtained woody area index (WAI) using DHP during leafless dates (i.e., May 1 and October 21) and assumed that the contribution of WAI to LAI was unchanged in leafy dates (i.e., the seasonal changes of the contribution of WAI to LAI was ignored); thus, the α in each date was derived accordingly from α = WAI/L_e, where WAI is the mean value of May 1 and October 21, L_e is the effective LAI estimated by DHP at that date.

Scheme B: We calculated the α value in each date based on the Photoshop software (PS). First, we obtained L_e of the photograph in a date using the DHP software. Second, the Clone Stamp Tool in PS was used to replace green materials (mainly leaves and needles) with sky, leaving just tree trucks and big branches on the images. Then we could obtain the WAI of the photograph using the DHP software again. Finally, the α value was then derived accordingly (α = WAI/L_e).

The Ω_E value for each photograph during all dates was calculated based on the Chen and Cihlar (CC) method (Chen and Cihlar, 1995b; Leblanc, 2002), which was frequently obtained via DHP-TRAC software. For each photograph during all dates, we corrected the systematic error caused by incorrect automatic photographic exposure based on the relationship between DHP L_e obtained with automatic exposure and LAI-2000 L_e reported by Zhang et al. (2005) and derived the E value accordingly.

2.4. Direct LAI estimation

2.4.1. Litter trap observations

At the study site, the litter (leaves, branches, seeds, etc.) captured by traps was recovered on August 1, and 15, September 1, 11, and 21, October 1, 11, and 21 in 2012. During each litter collection date, the leaves in each trap were sorted and weighed by species. After oven-drying the leaves at 65 °C for 48 h, we measured the weight of dried leaves. By multiplying the weight of each species by the specific leaf area (SLA), we estimated the total leaf area of the fallen leaves of each species at the time of sampling. To determine the SLA of each species, we sampled the leaves of each major species in August, September and October. The area of each sample leaf was measured through scanning using a BenQ-5560 image scanner (BenQ Corporation, China, 300 dpi resolutions). The areas of sample leaves were recorded, and the samples were then dried to a constant weight and weighed to the nearest milligram. Then the SLA for each species derived accordingly based on its definition (i.e., leaf area per unit of dry biomass). For a litter trap, we calculated the total leaf area of the fallen leaves of all species from August 1 to October 21, and then divided this value by the area of a litter trap to derive $\mathrm{LAI}_{\max}$.

2.4.2. Seasonal changes of LAI in leaf-out seasons

We conducted leaf seasonality observations by means of periodic *in situ* observations of sample shoots. We selected 15 shoots of 15 individuals of five species (i.e., three individuals of each species) for these samples at the study site. The selection of the five species was based on their relative rank in terms of the total tree basal area for the plot, and they included *Ulmus japonica*, *Betula platyphylla*, *Fraxinus mandshurica*, *Acer mono* and *Syringa reticulata*. On May 1, 12, 21, and 28, June 4, 12, and 22, July 5 and 15, and August 1 in 2012, we measured the number and size (length and width) of all leaves on each shoot. However, the area of a single leaf is not easily obtained from its length and width due to irregular shapes of leaves. Thus, we calculated the area per leaf using an adjustment coefficient based on the product of the length and width of a single leaf. To obtain the value of the adjustment coefficient for each species, 90 mature leaves were collected from each species in July to take the maximum length and width measurements of each sample leaf. Then the area of each sample leaf was measured by scanning and divided by the product of the length and width of this sample leaf to obtain the adjustment coefficient. We assumed that the value of the adjustment coefficient for each species did not change during the entire leaf-out season, and the values are given in Liu et al. (2015). Then, we could obtain the mean area per leaf for each species in each leaf-out season.

In this study, the unit of replication is the litter trap, and the average behavior of sample shoots of each species was applied to litterfall for all 20 litter traps. We assumed that the total number of leaves emerged during all leaf-out seasons equaled to the total number of fallen leaves of all leaf-fall seasons. In this case, once the mean area per leaf and the number of leaves of each species in a litter trap during each leaf-out season were obtained, we could estimate the LAI of each species for each sample point.

We assumed that the fallen leaves were all mature in leaf-fall seasons (i.e., the leaves do not grow in leaf-fall seasons), and the area per leaf for most species peaked in mid-July, thus, this date was considered as a mature period of leaves in this study. Then, the total number of fallen leaves of the entire leaf-fall season (N_{total}) for each species in a litter trap can be obtained from:

$$N_{total} = \frac{\sum_{t1}^{t2}\mathrm{SLA}\times W(t)}{\mathrm{LA}_{mature\text{-}mean}} \quad (4)$$

where SLA is the mean SLA for each species, $W(t)$ is the weight of fallen leaves in time t, where $t1$ = August 1, $t2$ = October 21, and $LA_{mature\text{-}mean}$ is the mean area per leaf in the mature period of leaves (i.e., July 15) for each species. We prior assumed that no leaves fell in the leaf-out season, thus we obtained the number of leaves for each species in a litter trap in time t ($n(t)$) from:

$$n(t) = N_{total} \times \frac{n_{shoot}(t)}{n_{shoot\text{-}max}} \quad (5)$$

where N_{total} was defined in Eq. (4), n_{shoot} (t) is the total number of leaves of a shoot in time t, $n_{shoot\text{-}max}$ is the annual maximum total number of leaves of a shoot, which produced in mid-July for each major species. Finally, the seasonal changes of LAI in time t (LAI (t)) for a forest plot during the leaf-out season were obtained from:

$$\mathrm{LAI}(t) = \frac{\sum \mathrm{LA}_i(t) \times n_i(t)}{A_{trap}} \quad (6)$$

where LA_i (t) is the mean area per leaf for species i in time t, n_i (t) is the number of leaves for species i in time t, and A_{trap} is the area of a litter trap.

2.4.3. Seasonal changes of LAI in leaf-fall seasons

When we obtained the $\mathrm{LAI_{max}}$ by adding the area of the fallen leaves from August 1 to October 21, we were also able to estimate the component LAI at each point between these dates for the leaf-fall season. Finally, the LAI for each plot was derived, from the initial leaf emergence date to the final leaf fall date. In this study, the LAI derived by combining the leaf seasonality observations and litter trap data were defined as direct LAI (LAI_{dir}).

2.5. Empirical models of direct LAI and effective LAI

In order to avoid the results of empirical models being affected by spatial autocorrelation, we first did a correlation analysis among the DHP LAIs by geostatistics software GS + 9.0 (Gamma Design Software, LLC, 2012) in the four plots for each date. We averaged the DHP LAIs with the distance less than 10 m if all sample points had significant spatial autocorrelation, i.e., (sill-nugget)/sill $\geqslant$ 0.25 (Zhang et al., 2011), where sill represents the total variation, and nugget represents the random variation. Subtraction of the random variation from the total variation results in the autocorrelated variation. Thus, (sill-nugget)/sill represents the proportion of the autocorrelated spatial heterogeneity in the total variation (Li and Reynolds, 1995). This geostatistical analysis was repeated to check if the combined sample points still had significant spatial autocorrelation, and some points with distance less than 15 m were further combined. The direct LAI measurements at the same points were also combined in the same way.

We constructed empirical relationships between LAI_{dir} and DHP L_e using three different methods based on linear models. First, we separated the entire growing season into 15 periods of about 10 days each and constructed a 10-day model for each date. Second, we ignored the seasonal changes in LAI and constructed an entire-season model relating LAI_{dir} to DHP L_e for the entire growing season. Third, we combined the above two methods: we first constructed an empirical model using the combined data for May 12 and May 21; for the two dates, we performed a paired-samples t test at the 95% significance level to determine whether there were significant differences between LAI_{dir} and estimated LAI using the empirical model. The idea was that, if there were no significant differences on both May 12 and 21, we would combine the data of May 12, 21 and 28 and carry out a paired-samples t test again; if there was a significant difference between LAI_{dir} and estimated LAI using the empirical model in just one date (May 12 or May 21), indicating that this model is not useful for the two dates, then we would combine the data from May 12 and May 28 and perform a paired-samples t test. By analogy, we continued this iteration until we had clearly grouped data with no significant differences together and kept those with significant differences apart. An empirical model was constructed using the data on LAI_{dir} and DHP L_e with no significant differences. The

Table 2
The seasonality of clumping index (Ω_E) and woody-to-total area ratio (α) in the four forest plots.

Month-day	Clumping index (Ω_E)	Woody-to-total area ratio (α)	
		Scheme A	Scheme B
5–12	0.88 (0.05)	0.64 (0.11)	0.45 (0.09)
5–21	0.92 (0.03)	0.38 (0.08)	0.16 (0.02)
5–28	0.92 (0.03)	0.27 (0.06)	0.07 (0.01)
6–4	0.94 (0.03)	0.26 (0.04)	0.08 (0.01)
6–12	0.92 (0.04)	0.28 (0.04)	0.07 (0.01)
6–22	0.89 (0.04)	0.24 (0.03)	0.05 (0.00)
7–5	0.88 (0.04)	0.25 (0.04)	0.05 (0.01)
7–15	0.88 (0.04)	0.26 (0.04)	0.04 (0.01)
8–1	0.91 (0.04)	0.24 (0.04)	0.05 (0.01)
8–16	0.93 (0.05)	0.24 (0.05)	0.04 (0.01)
9–1	0.94 (0.03)	0.28 (0.04)	0.07 (0.01)
9–11	0.93 (0.03)	0.29 (0.04)	0.10 (0.02)
9–21	0.94 (0.04)	0.32 (0.03)	0.13 (0.02)
10–1	0.96 (0.01)	0.55 (0.09)	0.33 (0.08)
10–11	0.94 (0.02)	0.89 (0.14)	0.69 (0.12)

Values in parentheses are standard deviations.

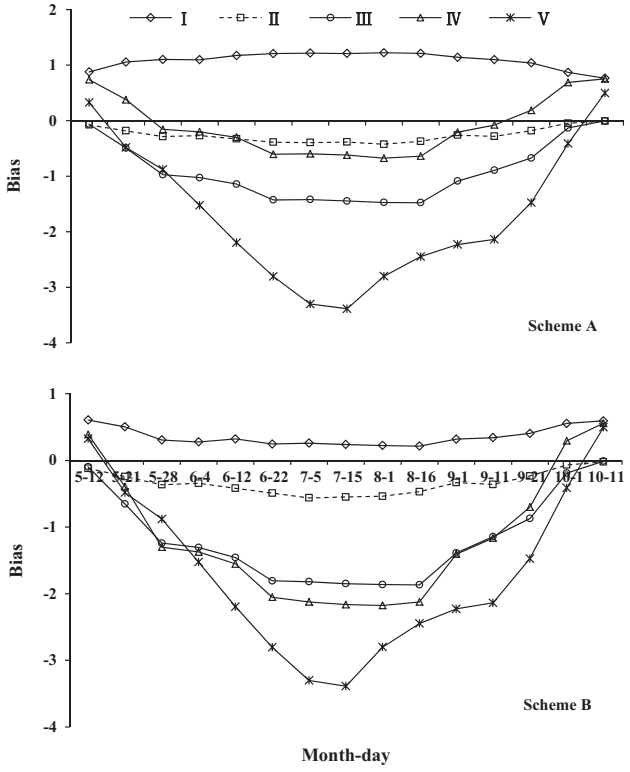

Fig. 1. The seasonal variations of the bias due to woody materials, clumping effects and automatic exposure, and the difference between effective LAI from DHP (DHP L_e) and direct LAI (LAI_{dir}). Scheme A: the bias of DHP L_e caused by woody materials was calculated using Scheme A, which the seasonal changes of the contribution of woody materials to optical LAI was ignored, and Scheme B: the bias of DHP L_e caused by woody materials was calculated using Scheme B, which that seasonal changes were considered. I: the bias due to woody materials, II: the bias due to clumping effects, III: the bias due to automatic exposure, IV: the total bias due to woody materials, clumping effects and automatic exposure, and V: the difference between DHP L_e and LAI_{dir}, which equals DHP L_e–LAI_{dir}.

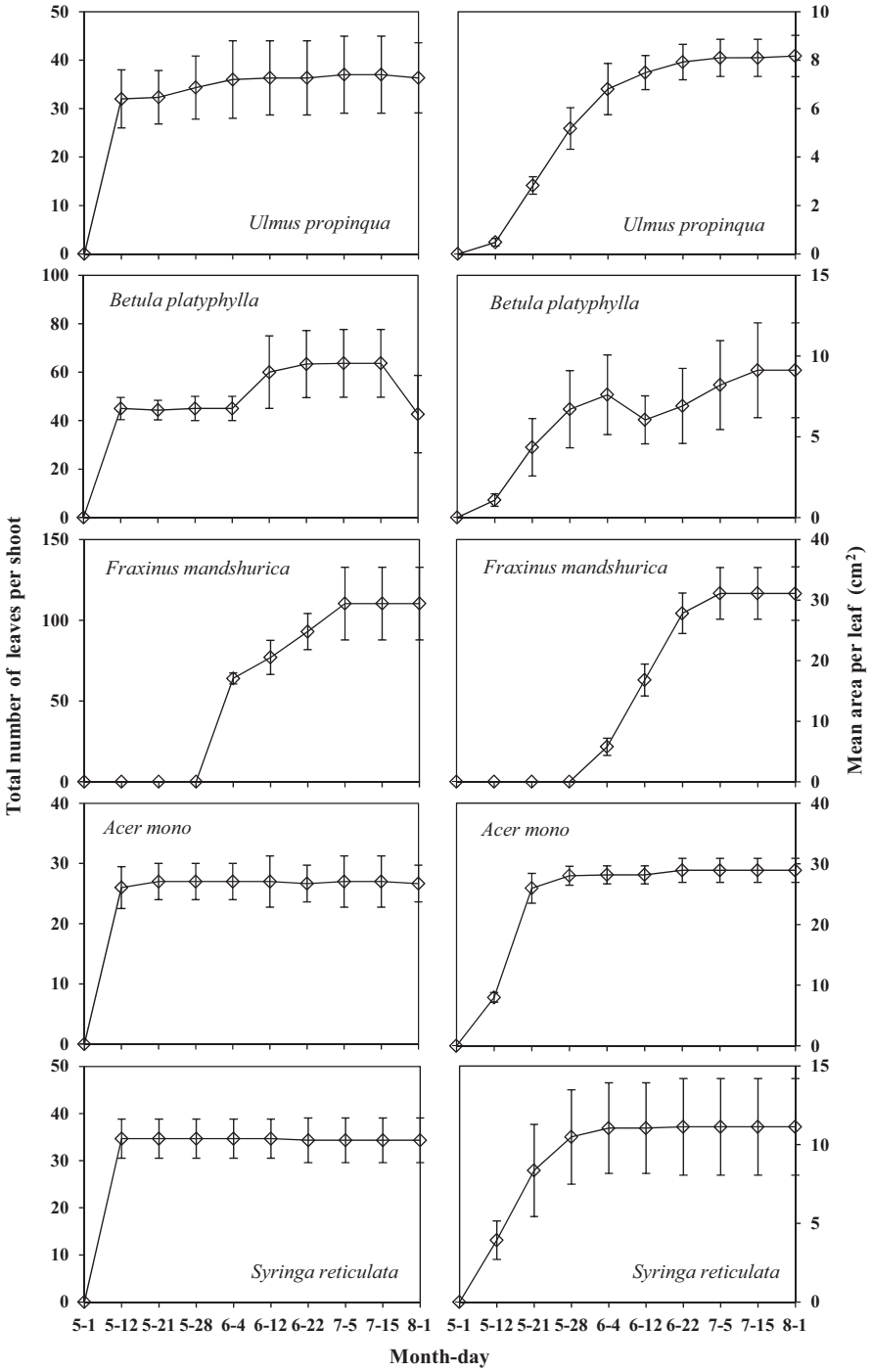

Fig. 2. Seasonality of leaf characteristics for the major species. Error bars represent the standard deviation.

model derived from the third method was defined as an aggregated model in this study. Finally, we used the LSD multiple comparison test to compare LAI_{dir} and estimated LAI using the three different methods in each date.

3. Results

3.1. The seasonality of canopy attributes and bias analysis

The Ω_E value in deciduous broadleaf forests did not show a clear seasonal variation (Table 2), and small standard deviation values indicate that the four forest plots exhibit similar canopy characteristics. The α value from scheme A and scheme B all showed clear seasonal variations, and the values from scheme A were larger than those from scheme B in each date (Table 2).

DHP L_e was larger than LAI_{dir} by 0.3 and 0.5 on May 12 and October 11, respectively, most likely because the contribution of woody materials to LAI is larger than that of leaves in these dates (Fig. 1). In contrast, DHP L_e was lower than LAI_{dir} by 0.4–3.4 from May 21 to October 1. Generally, the contribution of α to DHP L_e was opposite with other factors (e.g., Ω_E, or E), with weak seasonal variations in contrast to that of Ω_E and E (Fig. 1). For DHP L_e, the bias due to automatic exposure showed significantly seasonal variations in the ranges of $-1.5 \sim -0.1$ and $-1.9 \sim -0.1$ for scheme A

and scheme B, respectively. For scheme A, the total bias caused by α, Ω_E, and E was not sufficient to explain the difference between DHP L_e and LAI_{dir} during each date, probably because the contribution of woody materials to DHP L_e was exaggerated significantly. For scheme B, the total bias caused by α, Ω_E, and E could explain about 72% of the difference between DHP L_e and LAI_{dir} on average in the entire growing season. However, 36% of the difference (with a mean value of 1.1) between DHP L_e and LAI_{dir} could not be explained by α, Ω_E, and E in scheme B in July, probably because the contributions of clumping effects within canopies and incorrect automatic exposure to optical LAI were not adequately quantified in this study. These results suggest that it is difficult to obtain the accurate LAI for each season by correcting the DHP L_e for the above influence factors using current methods.

3.2. Leaf seasonality observations

All species exhibited pronounced seasonality of the total number of leaves per shoot and the mean area per leaf (Fig. 2). The leaves of most species emerged in early May, except for *F. mandshurica*, whose leaves emerged in late May. The total number of leaves per shoot (left column of Fig. 2) showed that most species (except *B. platyphylla* and *F. mandshurica*) experienced a single flush of leaf emergence (i.e., a rapid emergence of leaves) in early May, and this flush occurred over approximately two weeks. For example, more than 89%, 96% and 99% of total leaves had emerged by May 12 for *U. propinqua*, *A. mono* and *S. reticulata*, respectively. In contrast, *B. platyphylla* exhibited two leaf flushes: the first in early May and the second in early June. Because of the small area of the new leaves that emerged during the second flush, the mean area per leaf of *B. platyphylla* decreased in June, but it recovered with the growth of those small leaves from the second flush in early July. For *F. mandshurica*, the new leaves emerged successively in late May. In general, the number of leaves per shoot and mean area per leaf peaked in mid-July for all species. Unlike other species, *B. platyphylla* leaves began to fall after mid-July, and the fallen leaves accounted for 33% of the total leaves in early August.

3.3. Litter trap observations

Generally, leaves in each plot experienced a flush of leaf fall after September 21, and lasted for about two weeks (Fig. 3). The leaf mass for each plot was zero on October 31, indicating that the leaf fall finishes on October 21. The total leaf area from litter of all species collected throughout the leaf-fall season was 6.06 m^2 for each litter trap, and the leaf areas of major species exhibited clear differences (Table 3). In general, the leaf area of *U. propinqua* accounted for the largest proportion (27.3%) of the total leaf area of all species, followed by *B. platyphylla* and *F. mandshurica*, with proportions of 22.4% and 19.6%, respectively.

3.4. LAI empirical models

For each date, a significant correlation ($p < 0.01$ or $p < 0.05$, except $p = 0.052$ on July 15) was observed between LAI_{dir} and DHP L_e (Fig. 4), and the R^2 values ranged from 0.48 to 0.83 for all dates. Fig. 5 showed that DHP L_e was significantly correlated with LAI_{dir} over the entire growing season ($R^2 = 0.87$, RMSE = 0.24, $p < 0.01$). After combining the above two methods, we aggregated the empirical models into four formats (Fig. 6): Aggregated model A, including the dates of May 12 and 21, June 4, August 1 and 16; Aggregated model B, including the dates of May 28 and October 1; Aggregated model C, including the dates of June 12 and 22, September 1, 11 and 21; and Aggregated model D, including the dates of July 5, 15 and October 11. For the four aggregated models, LAI_{dir} and DHP L_e was significantly ($p < 0.01$) correlated with each other, with R^2 and RMSE values of 0.91 and 0.22, 0.79 and 0.29, 0.81 and 0.14, 0.97 and 0.14 for aggregated models A, B, C, and D, respectively.

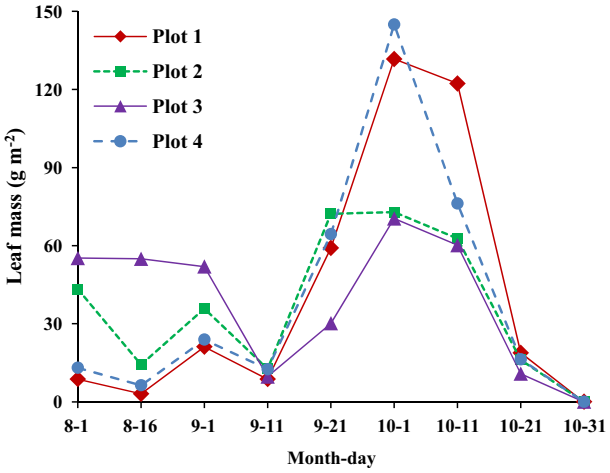

Fig. 3. The total leaf mass of all species in each litter collection date for the four plots. There was no litterfall in traps on October 31, indicating that the LAI of canopy is zero after last litter collection date (i.e., October 21), thus October 31 was outside of other study dates.

Fig. 7 illustrated the seasonal variations of LAI_{dir} and estimated LAI using the 10-day models, the entire-season model, and the aggregated models. Clearly, the data for each LAI format indicated that the LAI variation was dynamic over time. LAI_{dir} was highest on July 15 (6.06) and lowest on October 11 (0.25). From May 12 to June 4, LAI_{dir} increased rapidly—the average LAI_{dir} increased from 0.70 to 4.00, indicating that most leaves emerged and grew in this date. In contrast, LAI_{dir} decreased from July 15 to September 21, albeit slowly. From September 21 to October 11, LAI_{dir} decreased rapidly—the average LAI_{dir} decreased from 3.48 to 1.61, indicating that the rate of leaf fall is highest from September 21 to October 1.

Based on effective LAI, the estimated LAI using the 10-day model was very close to the LAI_{dir} in each date (Fig. 7), but there were so many models (Fig. 4) and the estimation process was so complicated that the models were not suitable for estimating the seasonal dynamics of LAI. On the other hand, the use of the entire-season model (Fig. 5) made the estimation process simple, but this model was not always effective in estimating the seasonal changes in LAI. For instance, there were significant differences ($p < 0.01$) between direct and estimated LAI by the entire-season model for May 28, June 4, October 1 and October 11 (Fig. 7). Considering the advantages and disadvantages of the empirical models for each date and for the entire growing season, we therefore combined the two methods. Fig. 6 showed the results of this aggregation as well as the empirical models, and Fig. 7 showed that there were no significant differences between LAI_{dir} and the

Table 3
Total leaf area from litter of the major species for each litter trap at the study site in the entire leaf-fall season.

Species	Total leaf area (m^2)	Proportion (%)
Ulmus propinqua	1.66 (0.31)	27.3
Betula platyphylla	1.36 (0.37)	22.4
Fraxinus mandshurica	1.18 (0.21)	19.6
Acer mono	0.53 (0.14)	8.8
Syringa reticulata	0.49 (0.12)	8.1
Others	0.83 (0.15)	13.7
Total	6.06	100

Values in parentheses are standard error. Number of litter traps $n = 20$.

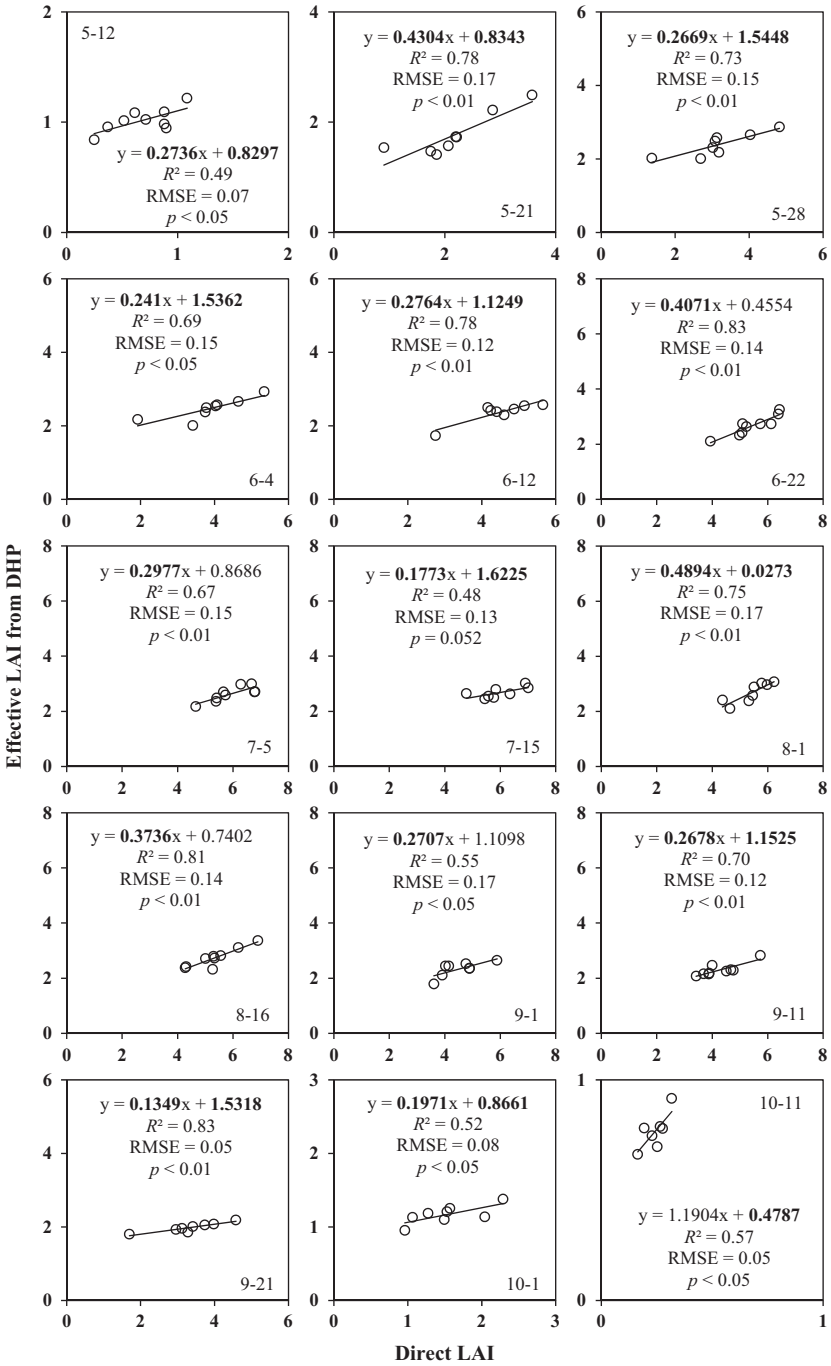

Fig. 4. 10-day models between direct LAI and effective LAI from DHP in the entire growing season. Highlighted in bold in empirical relationships are the intercepts for which the 95% confidence interval includes 0, and slopes that do not significantly differ from 1 ($p < 0.05$).

estimated LAI from the aggregated models in any date ($p < 0.01$), indicating that they were in good agreement in the estimation of the seasonal dynamics of LAI.

4. Discussion

4.1. LAI estimation by optical methods

Although LAI values derived from optical (i.e., indirect) methods usually need to be checked against direct LAI, optical methods are frequently used for the estimation of LAI in forest stands because of their convenience and effectiveness (Chen, 1996; Kalácska et al., 2005; Mason et al., 2012). Constructing an empirical model based on the correlation between direct LAI and optical LAI in different seasons could enable rapid and efficient determination of the seasonal changes in LAI by optical methods (e.g., DHP), which is very essential for modeling forest growth (Macfarlane et al., 2007) and validating global biophysical products derived from remote sensing data (Garrigues et al., 2008; Gonsamo and Pellikka, 2012; Majasalmi et al., 2013).

If the seasonal changes of the contribution of woody materials to optical LAI are ignored (i.e., scheme A), the total bias due to α, Ω_E, and E was far lower than the difference between DHP L_e and LAI_{dir} during most study dates, suggesting that a simple subtraction of WAI from DHP L_e would not always be appropriate, as already reported by others (Dufrêne and Bréda, 1995; Kucharik et al.,

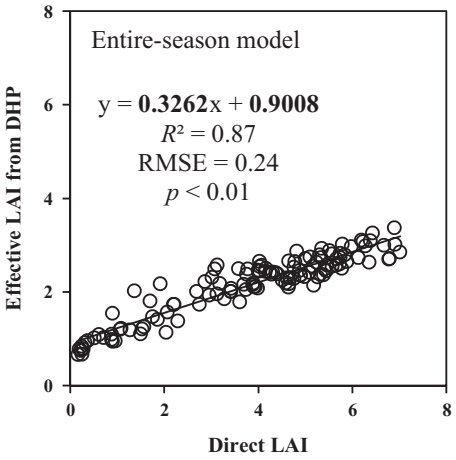

Fig. 5. Entire-season model between direct LAI and effective LAI from DHP. Highlighted in bold in the empirical relationship are the intercept for which the 95% confidence interval includes 0, and slope that do not significantly differ from 1 ($p < 0.05$).

1998; Barclay et al., 2000). For scheme B, the error caused by automatic exposure explained most of the difference between DHP L_e and LAI_{dir}, indicating that the photographic exposure should be set carefully in making DHP measurements. Although the seasonal changes of the contribution of woody materials to optical LAI was quantified based on PS and resulted in the total bias due to α, Ω_E, and E explained most of the difference between DHP L_e and LAI_{dir}, still about 28% of that difference was generally uncertain in the entire growing season. Despite the error caused by automatic exposure was considered in this study, the uncertainty is still mainly caused by incorrect photographic exposure in our opinion. Therefore, a method for effectively quantifying the seasonal variations of errors caused by automatic exposure in estimating LAI by DHP in deciduous broadleaf forests need to be addressed in future studies.

4.2. LAI estimation by the direct method

Leaf seasonality observations and SLA for major species are the two most important factors for estimating the seasonal changes in LAI_{dir} by the proposed method. The selection of more sampling species for leaf seasonality observations yields more accurate results. In this study, five species were selected for this purpose that accounted for more than 86% of the LAI_{max} estimated from the litter trap data. Thus, to attain more accurate estimates of the seasonality of LAI in the leaf-out season, we should obtain observations for more species that were ignored in this study. Jurik et al. (1985) reported that the SLA was the largest uncertainty in LAI estimates derived from the litter collection method because SLA varies with species and season (Nouvellon et al., 2010; Ishihara and Hiura, 2011; Majasalmi et al., 2013), which was taken into account in this study. To avoid the error caused by the spatial variation of SLA in estimating LAI, the species-specific SLA for each forest plot was used to estimate LAI.

In this study, we assessed the error of this direct method in different dates. For the LAI_{dir} during each leaf-out season, the bias was mainly caused by the measurements of the area per leaf and the total number of leaves for each major species; based on bias analysis (Topping, 1972), we obtained the total error of this method due to the two factors ranged from 4.3% to 9.6% during the whole leaf-out season. For the LAI_{dir} during each leaf-fall season, the bias was mainly caused by the measurements of SLA and mass of

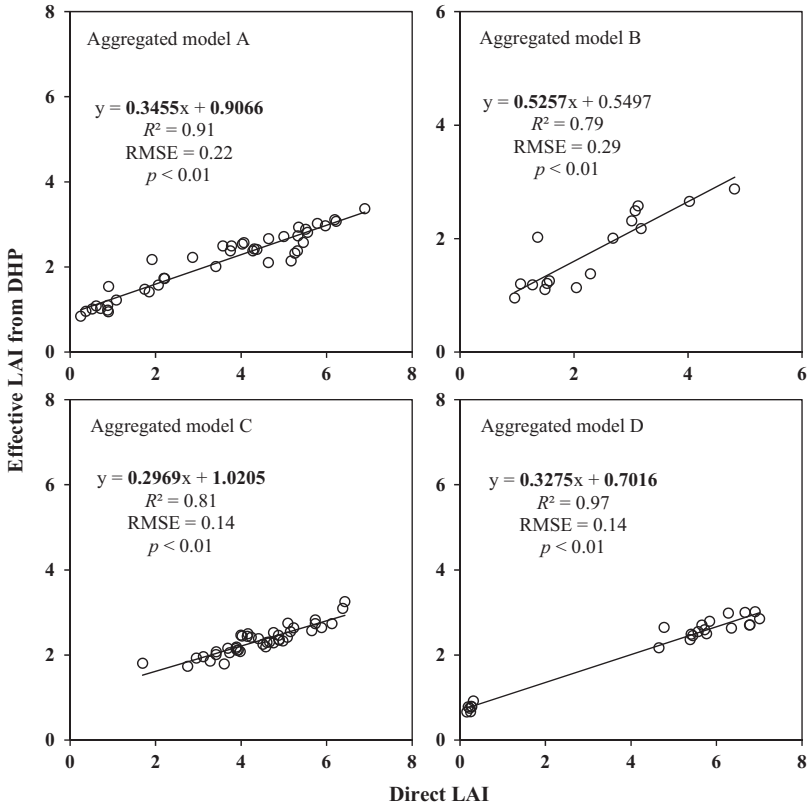

Fig. 6. Aggregated models between direct LAI and effective LAI from DHP. A, group of May 12 and 21, June 4, August 1 and 16; B, group of May 28 and October 1; C, group of June 12 and 22, September 1, 11 and 21; and D, group of July 5, 15 and October 11. Highlighted in bold in empirical relationships are the intercepts for which the 95% confidence interval includes 0, and slopes that do not significantly differ from 1 ($p < 0.05$).

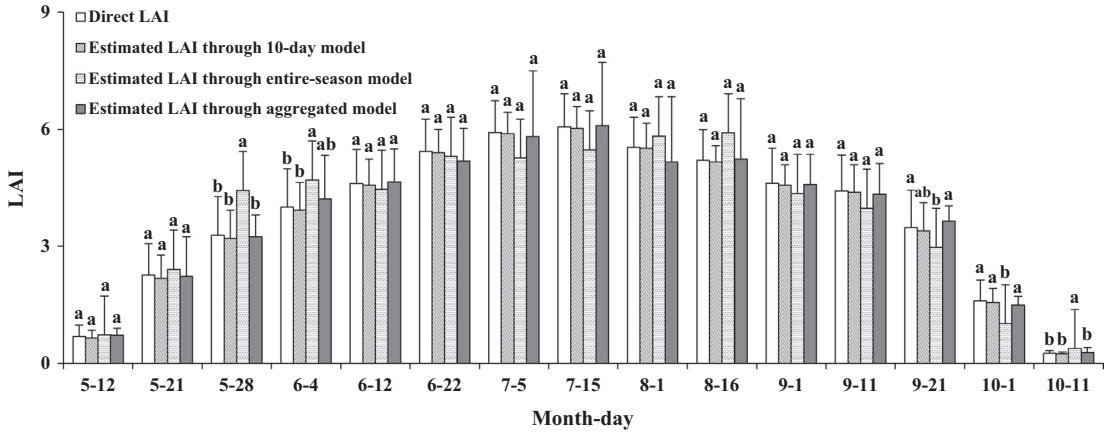

Fig. 7. Seasonal dynamics of LAI derived from different methods in the entire growing season in deciduous broadleaf forests. Different lowercase letters in the same date indicate a significant difference among LAI types at the 0.01 significance level.

litterfall for each major species, and we obtained the total error of this method due to the two factors ranged from 5.1% to 8.3% during the whole leaf-fall season.

Although the proposed method is able to directly estimate the seasonal variations in LAI by both the whole plot and each major species, it has some drawback. For instance, the proposed method is more applicable to deciduous canopies consisting of relatively small trees, because we only selected small trees for leaf seasonality observations in leaf-out seasons for convenience of measurements, i.e., we did not validate whether small trees and tall trees show similar leaf growth patterns in this study, which will be addressed in further studies.

4.3. Comparison with indirect and direct methods of LAI estimation

The optical method generally underestimated the LAI in deciduous forest stands, as reported in many previous studies (Cutini et al., 1998; Eriksson et al., 2005; Chianucci and Cutini, 2013). However, whether this underestimation trend varies with season has rarely been reported. Our results clearly showed that the difference between DHP L_e and LAI_{dir} had strong seasonal variations (Fig. 1). DHP L_e underestimated LAI_{dir} at most study dates (i.e., from May 21 to October 1), and this underestimation increased with increasing LAI values, probably because (1) the bias due to woody materials decreased, because part of woody materials was masked by increasing leaves, (2) the bias due to clumping effects within canopies increasing with leaf growth, and (3) the bias due to automatic exposure increased with the increasing leaves in canopies. In contrast, DHP L_e overestimated LAI_{dir} in the early leaf-out (e.g., May 12) and late leaf-fall seasons (e.g., October 11), primarily due to the contribution of woody materials to LAI because there were few leaves at these dates.

Indirect LAI is significantly correlated with direct LAI in deciduous forests, as previously noted by numerous authors (Gower and Norman, 1991; Dufrêne and Bréda, 1995; Cutini et al., 1998). In general, we also found a significant relationship between direct LAI and optical (DHP) LAI (Fig. 5). However, the entire-season model was not always useful for estimating LAI based on DHP in each date (Fig. 7). This most likely results from the large changes in LAI at the beginning and end of the growing season, i.e., the rapid increase from 2.26 to 4.00 from May 21 to June 4 and the linear decrease from 4.42 to 0.25 from September 11 to October 11. Therefore, the entire-season model is unable to accurately and completely estimate the seasonal changes in LAI based on DHP. Although we could accurately estimate the seasonal changes in LAI using the 10-day models, this approach is complicated and time-consuming.

From a practical standpoint, the aggregated models are worthy of recommendation for estimating seasonal changes in LAI relative to the other two models (i.e., the 10-day models and the entire-season model). In our study, different 10-day models were merged into four aggregated models based not only on the data themselves but also on biological and ecological reasons. Aggregated model A was applicable to the dates of both early leaf emergence (e.g., May 12 and 21) and early leaf fall (e.g., August 1 and 16), most likely because of similar contributions of both woody materials and clumping effects in canopies to estimates of optical LAI at these times. The contribution of woody materials to optical LAI decreased with the growth of leaves because a portion of woody materials such as stems and branches was masked by the leaves; later, the woody contribution increased with leaf fall because more woody material was again visible (Barclay et al., 2000; Zou et al., 2009). In contrast, clumping effects exhibited an opposite temporal pattern in their contribution to optical LAI. The contribution of woody materials to optical LAI in the early leaf-out season was larger than in the early leaf-fall season, but the contribution of clumping effects in the early leaf-out season was smaller than in the early leaf-fall season. Thus, the total contribution of the two components (i.e., woody materials + clumping effects) might have been balanced in the early leaf-out vs. early leaf-fall seasons. Aggregated model B was useful for May 28 and October 1, two dates during which rapid changes in LAI occurred; the LAI on May 28 increased by 50% relative to May 21, and the LAI on October 1 decreased by 54% relative to September 21, so the DHP L_e in these two dates was underestimated by similar degrees (21% for May 28 and 19% for October 1). Aggregated model C worked well on June 12 and 22 and from September 1 to 21, most likely because these dates exhibited similar continuous changes in LAI as well as sharing similar direct LAIs, with a mean value of 4.51 (SD = 0.70). Aggregated model D was suitable for July 5, July 15 and October 11 because the former two date exhibits stable LAI, with values of 5.91 and 6.06, respectively, and October 11 was also included without an obvious explanation, perhaps because of the data themselves. The seasonal changes in LAI in broadleaf forests found in our study have been reported by previous studies in various forests around the world, even in tropical regions (Wang et al., 2005; Heiskanen et al., 2012; Potithep et al., 2013). However, we also found that the relationship between direct LAI and optical LAI changes due to variable seasonal influences of various parameters on LAI, as reported by other researchers (e.g., Qi et al., 2013; Tillack et al., 2014). Therefore, to accurately estimate seasonal

changes in LAI based on optical measurements, these variable influences should be considered in similar forests in future research. In addition, the four aggregated models are able to fully explain the seasonal variations in LAI from initial leaf emergence to leaf fall, and therefore their use can allow rapid and reliable estimation of LAI in different dates during the growing season.

5. Conclusions

We have estimated the seasonal changes of LAI using direct and indirect (DHP) methods in deciduous broadleaf forests. We also evaluated the seasonal variations of the biases in DHP L_e due to the woody materials, clumping effects and automatic exposure, and the total biases caused by these factors explained 72% of the difference between LAI_{dir} and DHP L_e during the entire growing season. Since these biases varied seasonally, we first separated the growing season into 15 periods of about 10 days each and then regressed DHP L_e against LAI_{dir} for each 10-day period. Based on these regressions, we found that regression models for four aggregated periods performed as well as the 10-day models. In this way, the DHP measurement can be rapidly and reliably converted into the LAI_{dir} for entire growing season from the initial leaf emergence to leaf fall. These regression models would be applicable to forests of similar characteristics.

Acknowledgments

We would like to express our gratitude to the editor and anonymous reviewers for their constructive and valuable comments concerning the manuscript. This work was financially supported by the Ministry of Science and Technology of China (No. 2011BAD37B01).

References

Arias, D., Calvo-Alvarado, J., Dohrenbusch, A., 2007. Calibration of LAI-2000 to estimate leaf area index (LAI) and assessment of its relationship with stand productivity in six native and introduced tree species in Costa Rica. For. Ecol. Manage. 247, 185–193.
Asner, G.P., Scurlock, J.M.O., A Hicke, J., 2003. Global synthesis of leaf area index observations: implications for ecological and remote sensing studies. Glob. Ecol. Biogeogr. 12, 191–205.
Barclay, H., Trofymow, J., Leach, R., 2000. Assessing bias from boles in calculating leaf area index in immature Douglas-fir with the LI-COR canopy analyzer. Agric. For. Meteorol. 100, 255–260.
Beckschäfer, P., Seidel, D., Kleinn, C., Xu, J., 2013. On the exposure of hemispherical photographs in forests. iForest-Biogeosci. Forest. 6, 228–237.
Black, T.A., Chen, J.M., Lee, X., Sagar, R.M., 1991. Characteristics of shortwave and longwave irradiances under a Douglas-fir forest stand. Can. J. For. Res. 21, 1020–1028.
Bréda, N.J.J., 2003. Ground-based measurements of leaf area index: a review of methods, instruments and current controversies. J. Exp. Bot. 54, 2403–2417.
Chason, J.W., Baldocchi, D.D., Huston, M.A., 1991. A comparison of direct and indirect methods for estimating forest canopy leaf area. Agric. For. Meteorol. 57, 107–128.
Chen, J.M., 1996. Optically-based methods for measuring seasonal variation of leaf area index in boreal conifer stands. Agric. For. Meteorol. 80, 135–163.
Chen, J.M., Black, T.A., 1992. Defining leaf area index for non-flat leaves. Plant, Cell Environ. 15, 421–429.
Chen, J.M., Black, T.A., Adams, R.S., 1991. Evaluation of hemispherical photography for determining plant area index and geometry of a forest stand. Agric. For. Meteorol. 56, 129–143.
Chen, J.M., Cihlar, J., 1995a. Plant canopy gap-size analysis theory for improving optical measurements of leaf-area index. Appl. Opt. 34, 6211–6222.
Chen, J.M., Cihlar, J., 1995b. Quantifying the effect of canopy architecture on optical measurements of leaf area index using two gap size analysis methods. IEEE Trans. Geosci. Remote Sens. 33, 777–787.
Chen, J.M., Rich, P.M., Gower, S.T., Norman, J.M., Plummer, S., 1997. Leaf area index of boreal forests: theory, techniques, and measurements. J. Geophys. Res. 102, 29429–29443.
Chianucci, F., Cutini, A., 2012. Digital hemispherical photography for estimating forest canopy properties: current controversies and opportunities. iForest-Biogeosci. Forest. 5, 290–295.
Chianucci, F., Cutini, A., 2013. Estimation of canopy properties in deciduous forests with digital hemispherical and cover photography. Agric. For. Meteorol. 168, 130–139.
Chianucci, F., Macfarlane, C., Pisek, J., Cutini, A., Casa, R., 2015. Estimation of foliage clumping from the LAI-2000 Plant Canopy Analyzer: effect of view caps. Trees 29, 355–366.
Cutini, A., Matteucci, G., Mugnozza, G., 1998. Estimation of leaf area index with the Li-Cor LAI-2000 in deciduous forests. For. Ecol. Manage. 105, 55–65.
Dufrêne, E., Bréda, N., 1995. Estimation of deciduous forest leaf area index using direct and indirect methods. Oecologia 104, 156–162.
Eriksson, H., Eklundh, L., Hall, K., Lindroth, A., 2005. Estimating LAI in deciduous forest stands. Agric. For. Meteorol. 129, 27–37.
Garrigues, S., Shabanov, N.V., Swanson, K., Morisette, J.T., Baret, F., Myneni, R.B., 2008. Intercomparison and sensitivity analysis of leaf area index retrievals from LAI-2000, AccuPAR, and digital hemispherical photography over croplands. Agric. For. Meteorol. 148, 1193–1209.
Gonsamo, A., Pellikka, P., 2009. The computation of foliage clumping index using hemispherical photography. Agric. For. Meteorol. 149, 1781–1787.
Gonsamo, A., Pellikka, P., 2012. The sensitivity based estimation of leaf area index from spectral vegetation indices. ISPRS J. Photogr. Remote Sens. 70, 15–25.
Gower, S.T., Kucharik, C.J., Norman, J.M., 1999. Direct and indirect estimation of leaf area index, f (APAR), and net primary production of terrestrial ecosystems. Remote Sens. Environ. 70, 29–51.
Gower, S.T., Norman, J.M., 1991. Rapid estimation of leaf area index in conifer and broad-leaf plantations. Ecology 72, 1896–1900.
Heiskanen, J., Rautiainen, M., Stenberg, P., Mõttus, M., Vesanto, V.H., Korhonen, L., Majasalmi, T., 2012. Seasonal variation in MODIS LAI for a boreal forest area in Finland. Remote Sens. Environ. 126, 104–115.
Ishihara, M.I., Hiura, T., 2011. Modeling leaf area index from litter collection and tree data in a deciduous broadleaf forest. Agric. For. Meteorol. 151, 1016–1022.
Jonckheere, I., Fleck, S., Nackaerts, K., Muys, B., Coppin, P., Weiss, M., Baret, F., 2004. Review of methods for in situ leaf area index determination: Part I. Theories, sensors and hemispherical photography. Agric. For. Meteorol. 121, 19–35.
Jonckheere, I., Muys, B., Coppin, P., 2005. Allometry and evaluation of in situ optical LAI determination in Scots pine: a case study in Belgium. Tree Physiol. 25, 723–732.
Jurik, T.W., Briggs, G.M., Gates, D.M., 1985. A comparison of four methods for determining leaf area index in successional hardwood forests. Can. J. For. Res. 15, 1154–1158.
Küßner, R., Mosandl, R., 2000. Comparison of direct and indirect estimation of leaf area index in mature Norway spruce stands of eastern Germany. Can. J. For. Res. 30, 440–447.
Kalácska, M., Calvo-Alvarado, J.C., Sanchez-Azofeifa, G.A., 2005. Calibration and assessment of seasonal changes in leaf area index of a tropical dry forest in different stages of succession. Tree Physiol. 25, 733–744.
Kucharik, C.J., Norman, J.M., Gower, S.T., 1998. Measurements of branch area and adjusting leaf area index indirect measurements. Agric. For. Meteorol. 91, 69–88.
Leblanc, S.G., 2002. Correction to the plant canopy gap-size analysis theory used by the Tracing Radiation and Architecture of Canopies instrument. Appl. Opt. 41, 7667–7670.
Leblanc, S.G., Fournier, R., 2014. Hemispherical photography simulations with an architectural model to assess retrieval of leaf area index. Agric. For. Meteorol. 194, 64–76.
Leblanc, S.G., Chen, J.M., Fernandes, R., Deering, D.W., Conley, A., 2005. Methodology comparison for canopy structure parameters extraction from digital hemispherical photography in boreal forests. Agric. For. Meteorol. 129, 187–207.
Li, H., Reynolds, J., 1995. On definition and quantification of heterogeneity. Oikos 73, 280–284.
Liu, Z.L., Wang, X.C., Chen, J.M., Wang, C.K., Jin, G.Z., 2015. On improving the accuracy of digital hemispherical photography measurements of seasonal leaf area index variation in deciduous broadleaf forests. Can. J. For. Res. (early view). http://dx.doi.org/10.1139/cjfr-2014-0351.
Macfarlane, C., Hoffman, M., Eamus, D., Kerp, N., Higginson, S., McMurtrie, R., Adams, M., 2007. Estimation of leaf area index in eucalypt forest using digital photography. Agric. For. Meteorol. 143, 176–188.
Macfarlane, C., Ryu, Y., Ogden, G.N., Sonnentag, O., 2014. Digital canopy photography: exposed and in the raw. Agric. For. Meteorol. 197, 244–253.
Majasalmi, T., Rautiainen, M., Stenberg, P., Lukeš, P., 2013. An assessment of ground reference methods for estimating LAI of boreal forests. For. Ecol. Manage. 292, 10–18.
Mason, E.G., Diepstraten, M., Pinjuv, G.L., Lasserre, J.-P., 2012. Comparison of direct and indirect leaf area index measurements of *Pinus radiata* D. Don. Agric. For. Meteorol. 166–167, 113–119.
Miller, J.B., 1967. A formula for average foliage density. Aust. J. Bot. 15, 141–144.
Nasahara, K.N., Muraoka, H., Nagai, S., Mikami, H., 2008. Vertical integration of leaf area index in a Japanese deciduous broad-leaved forest. Agric. For. Meteorol. 148, 1136–1146.
Neumann, H.H., Den Hartog, G., Shaw, R.H., 1989. Leaf area measurements based on hemispheric photographs and leaf-litter collection in a deciduous forest during autumn leaf-fall. Agric. For. Meteorol. 45, 325–345.
Nouvellon, Y., Laclau, J.P., Epron, D., Kinana, A., Mabiala, A., Roupsard, O., Bonnefond, J.M., Le Maire, G., Marsden, C., Bontemps, J.D., 2010. Within-stand and seasonal variations of specific leaf area in a clonal Eucalyptus plantation in the Republic of Congo. For. Ecol. Manage. 259, 1796–1807.

Potithep, S., Nagai, S., Nasahara, K.N., Muraoka, H., Suzuki, R., 2013. Two separate periods of the LAI–VIs relationships using in situ measurements in a deciduous broadleaf forest. Agric. For. Meteorol. 169, 148–155.
Qi, Y.J., Jin, G.Z., Liu, Z.L., 2013. Optical and litter collection methods for measuring leaf area index in an old-growth temperate forest in northeastern China. J. For. Res. 18, 430–439.
Richardson, A.D., Dail, D.B., Hollinger, D.Y., 2011. Leaf area index uncertainty estimates for model-data fusion applications. Agric. For. Meteorol. 151, 1287–1292.
Ross, J., 1981. The Radiation Regime and Architecture of Plant Stands. Junk, The Hague, 391.
Ryu, Y., Verfaillie, J., Macfarlane, C., Kobayashi, H., Sonnentag, O., Vargas, R., Ma, S., Baldocchi, D.D., 2012. Continuous observation of tree leaf area index at ecosystem scale using upward-pointing digital cameras. Remote Sens. Environ. 126, 116–125.
Smith, N., Chen, J., Black, T., 1993. Effects of clumping on estimates of stand leaf area index using the LI-COR LAI-2000. Can. J. For. Res. 23, 1940–1943.
Sprintsin, M., Cohen, S., Maseyk, K., Rotenberg, E., Grünzweig, J., Karnieli, A., Berliner, P., Yakir, D., 2011. Long term and seasonal courses of leaf area index in a semi-arid forest plantation. Agric. For. Meteorol. 151, 565–574.
Tillack, A., Clasen, A., Kleinschmit, B., Förster, M., 2014. Estimation of the seasonal leaf area index in an alluvial forest using high-resolution satellite-based vegetation indices. Remote Sens. Environ. 141, 52–63.
Topping, J., 1972. Errors of Observation and their Treatment. Chapman and Hall, London, England.
van Gardingen, P.R., Jackson, G.E., Hernandez-Daumas, S., Russell, G., Sharp, L., 1999. Leaf area index estimates obtained for clumped canopies using hemispherical photography. Agric. For. Meteorol. 94, 243–257.
Wang, C., Han, Y., Chen, J., Wang, X., Zhang, Q., Bond-Lamberty, B., 2013. Seasonality of soil CO_2 efflux in a temperate forest: biophysical effects of snowpack and spring freeze–thaw cycles. Agric. For. Meteorol. 177, 83–92.
Wang, Q., Adiku, S., Tenhunen, J., Granier, A., 2005. On the relationship of NDVI with leaf area index in a deciduous forest site. Remote Sens. Environ. 94, 244–255.
Zhang, Y., Chen, J.M., Miller, J.R., 2005. Determining digital hemispherical photograph exposure for leaf area index estimation. Agric. For. Meteorol. 133, 166–181.
Zhang, Z.H., Hu, G., Zhu, J.D., Ni, J., 2011. Spatial heterogeneity of soil nutrients and its impact on tree species distribution in a karst forest of Southwest China. Chin. J. Plant Ecol. 35, 1038–1049.
Zou, J., Yan, G., Zhu, L., Zhang, W., 2009. Woody-to-total area ratio determination with a multispectral canopy imager. Tree Physiol. 29, 1069–1080.